

Corrosion Mechanism of Alloy 600 in Aqueous $\text{Na}_2\text{S}_2\text{O}_3$ Solutions at 340°C

E. H. Lee, K. M. Kim, B. S. Choi, and W. Y. Maeng
Nuclear Materials Research Division, Korea Atomic Energy Research Institute,
1045 Daedeok Street, Yuseong, Daejeon 305-353, Korea
* ehlee@kaeri.re.kr

1. Introduction

Intergranular attack and stress corrosion cracking (IGA/SCC) of steam generator (SG) tubing materials have been observed in SG crevices, such as tube support plates, tube sheets, and sludge piles in pressurized water-reactor (PWR) plants. For the PWR plants, sulfur has been identified as one of the major impurities introduced into the secondary-side water of PWR [1]. One of the principal species identified after hideout return is sulfate (SO_4^{2-} , +6). Under SG operating conditions, SO_4^{2-} reduced to lower-valence sulfur species which are detrimental to metals and are found inside advancing SCC from the pulled tubes [2]. As one of the reduced sulfur species, thiosulfate ($\text{S}_2\text{O}_3^{2-}$, +2) is known to cause SCC of sensitized Alloy 600 and stainless steel [3]. In addition, this species also caused an accident of Three Mile Island Unit 1 power plant [3].

In the present work, we investigate the effects of $\text{S}_2\text{O}_3^{2-}$ concentrations on the corrosion behavior of Alloy 600 using SCC tests. And then, corrosion mechanisms of Alloy 600 with varying concentration of $\text{S}_2\text{O}_3^{2-}$ are described.

2. Methods and Results

2.1 Materials and Test Procedures

The material used was commercial Alloy 600 with a 22.23 mm outer diameter and a wall thickness of 1.27 mm. The tubing was mill-annealed at 960°C for 10 min. The chemical compositions of the material in wt% are as follows: 0.01 C, 73.1 Ni, 15.4 Cr, 8.0 Fe, 0.1 Si, 0.3 Mn, 0.2 Cu, 0.17 Ti, and 0.22 Al. We prepared test solutions using distilled water ($>17 \text{ M}\Omega\cdot\text{cm}$) with an addition of reagent-grade sodium thiosulfate ($\text{Na}_2\text{S}_2\text{O}_3$).

For the SCC tests, a shape, geometry of the sample, and preparation of test specimens are shown in our previous work [4]. We conducted the SCC tests in deaerated 0.005 M, 0.01 M, and 0.1 M $\text{Na}_2\text{S}_2\text{O}_3$ solutions using a static-autoclave system at 340°C and at corrosion potential. The test samples were inspected every 240 h and 480 h with a stereoscopic microscope to observe cracks. Cross-section samples prepared from the cracked test samples were examined with a scanning electron microscopy (SEM) to identify crack initiation and propagation. To determine the chemical compositions of the oxide layers, an energy dispersive X-ray system (EDS) was used. Deposits on the surfaces

of the test specimens were analyzed with a low angle X-ray diffractometer (XRD).

2.2 Corrosion Behaviors

The SCC susceptibilities of test samples increased with increasing concentration of $\text{S}_2\text{O}_3^{2-}$ for 0.005 M and 0.01 M $\text{S}_2\text{O}_3^{2-}$ solution. However, for 0.1 M $\text{S}_2\text{O}_3^{2-}$ solution, no SCC observed because of severe general corrosion. A scent of H_2S was identified after testing. The surfaces of the test samples were covered with thick, black deposits composed of mainly of nickel sulfide (Ni_3S_2). The fractured surfaces were covered with many impurities composed sulfur species which was confirmed by EDS and XRD analyses. Results of XRD analyses and the presence of scent of H_2S confirmed that the $\text{S}_2\text{O}_3^{2-}$ reduced to a lower-valence sulfur species in the absence of reducing agents. For 0.005 M $\text{S}_2\text{O}_3^{2-}$ solution, the test samples showed SCC after 3840 h and 4800 h. For 0.01 M $\text{S}_2\text{O}_3^{2-}$ solution, the results were shown in our previous work [4]. A severe general corrosion was observed in the 0.1 M $\text{S}_2\text{O}_3^{2-}$ solution, which is consistent with data from Brandy et al. [3].

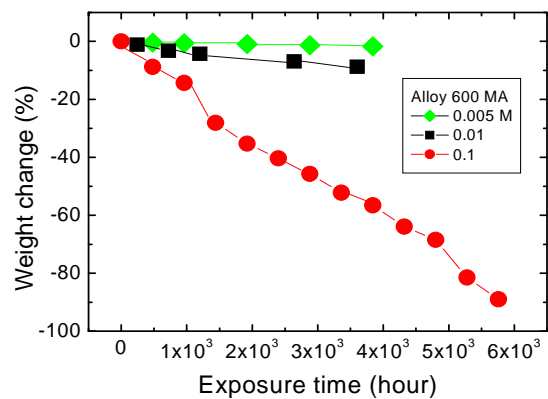


Fig. 1. The weight change measured on Alloy 600 specimens exposed in $\text{S}_2\text{O}_3^{2-}$ solutions.

Fig. 1 shows the weight change of the test samples with varying solution concentrations as a function of exposure time. For the 0.1 M $\text{S}_2\text{O}_3^{2-}$ solution, the test sample decreased in weight over 50 % from the original weight when the test samples in the 0.005 M and 0.01 M $\text{S}_2\text{O}_3^{2-}$ solutions were observed. For the $\text{S}_2\text{O}_3^{2-}$, an anodic dissolution increased significantly with increasing $\text{S}_2\text{O}_3^{2-}$ concentration. Bandy et al. reported

that $S_2O_3^{2-}$ can initiate SCC only when the material is severely sensitized [3]. However, in this work, the SCC was observed although the material was not sensitized.

2.3 Observations of Cross-section

The Fig. 2 (a) shows SEM image of the cross-section sample tested in the 0.005 M $S_2O_3^{2-}$ solution. Various lengths of small cracks appeared at the surfaces and an extended crack was as deep as $\sim 700 \mu\text{m}$ from the outer surface of the test sample. The outer, loosely bonded Ni_3S_2 layer was completely removed by sonication. An oxide layer with varying thickness is observed, and the existence of shallow peaks below this layer is noted. Many side cracks appeared along the open-crack walls. EDS profiles, in Fig. 2 (b), shows Cr-rich oxide layer, beneath which is a small sulfur peak, on one side of the crack walls. However, a Ni and sulfur-enrichment layer is shown on the other side of the crack walls.

Table 1 lists the results of the EDS analyses on labeled positions in Fig. 2 (a), which shows sulfur, iron and Cr enrichment on the both side of crack walls. Above results are consistent with results of our previous work in the 0.01 M $S_2O_3^{2-}$ solution, which revealed that sulfur and iron are present within the Cr oxide layer [4].

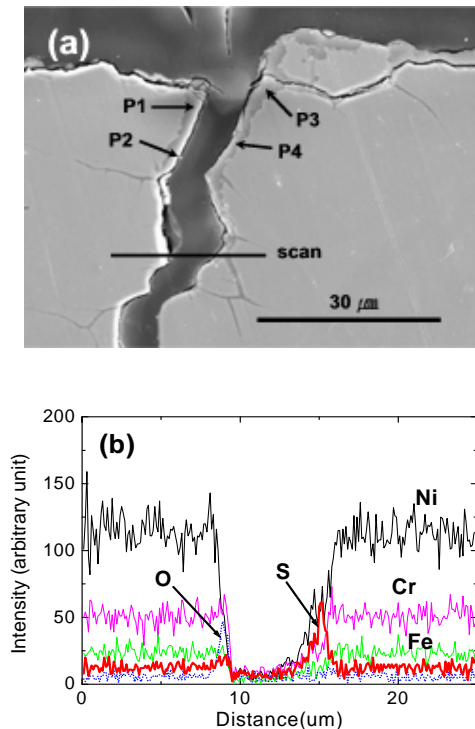


Fig. 2. Cross-section morphology (a) and EDS profiles across the crack (b).

In this work, the observed results suggest that first, elemental sulfur which is one of decomposing products of $S_2O_3^{2-}$ and other decomposed-sulfur oxy anions adsorb on the surface of the test samples. As a result,

the highly porous-oxide layer containing Cr-O-Ni-S-Fe forms. After forming oxide layers, sulfur in the oxide layer diffuse into the metal matrix along the grain boundaries. The incoming sulfur reacts with Ni near the grain boundaries to form Ni_3S_2 . With sulfur, the passive films containing Ni_3S_2 , Cr_2O_3 , $Cr(OH)_3$, and $Ni(OH)_2$ again form [5]. Before cracking the oxide layer completely, above process will be repeated and leads to SCC of the test samples. To identify the microstructure of the crack-wall oxide layer and crack-tip area, nanometer-resolution methods are needed.

Table 1. EDS results at P1-P4 labeled in Fig. 2 (a).

	P1	P2	P3	P4
S	1.93	6.40	4.78	1.54
Ni	21.90	29.95	23.63	25.08
O	34.69	18.34	32.64	36.41
Cr	30.28	29.85	28.45	24.62
Fe	11.19	15.46	10.50	12.36

3. Conclusions

In the deaerated 0.005 M and 0.01 M sodium thiosulfate solutions at 340°C , an IGSCC was observed. For the 0.1 M sodium thiosulfate solution, a general corrosion was observed. Reduction of thiosulfate to species of a lower valence was confirmed by the EDS profiles and XRD data. The corrosion mechanism of Alloy 600 is first, the adsorption of thiosulfate ions onto the metal surfaces to form passive films containing Ni, Cr, Fe, S, and O. After forming highly porous-oxide layers, sulfur in the oxide layer diffuses into the metal matrix along the grain boundaries to produce a SCC of the Alloy 600.

REFERENCES

- [1] O. Bouvier, B. Prioux, F. Vaillant, M. Bouchacourt, and P. Lemaire, Nickel Alloys Corrosion Cracking in Neutral and Lightly Alkaline Sulfate Environment, Proc. 9th Int. Symp. on Environmental Degradation of Materials in Nuclear Power System-Water Reactors, p. 567, 2002.
- [2] C. Laire, G. Blatbrood, and J. Stubbe, Characterization of the Secondary Side Deposits of Pulled Steam Generator Tubes, Proc. 7th Int. Symp. on Environmental Degradation of Materials in Nuclear Power System-Water Reactors, p. 387, 1995.
- [3] R. Bandy, R. Roberge, and R. C. Newman, Low Temperature Stress Corrosion Cracking of Inconel 600 under Two Different Conditions of Sensitization, Corrosion Science, Vol. 23, p. 995, 1983.
- [4] E. H. Lee, K. M. Kim, and U. C. Kim, Effects of Reduced Sulfur on the Corrosion Behavior of Alloy 600 in High-temperature Water, Materials Science & Engineering A, Vol. 449-451, p. 330, 2007.
- [5] P. Marcus and J. M. Grimal, The Antagonistic Roles of Chromium and Sulphur in the Passivation of Ni-Cr-Fe Alloys Studied by XPS and Radiochemical Techniques, Corrosion Science, Vol. 31, p. 377, 1990.